01 Jan 2023

Epitaxial Electrodeposition Of Ordered Inorganic Materials

Jay A. Switzer
Missouri University of Science and Technology, jswitzer@mst.edu

Avishek Banik

ACCOUNTS of chemical research

pubs.acs.org/accounts Article

Epitaxial Electrodeposition of Ordered Inorganic Materials

Published as part of the Accounts of Chemical Research special issue "Electrosynthesis of Inorganic Materials".

Jay A. Switzer* and Avishek Banik

Cite This: https://doi.org/10.1021/acs.accounts.3c00007 Read Online

ACCESS | Metrics & More | Article Recommendations

CONSPECTUS: The quality of technological materials generally improves as the crystallographic order is increased. This is particularly true in semiconductor materials, as evidenced by the huge impact that bulk single crystals of silicon have had on electronics. Another approach to producing highly ordered materials is the epitaxial growth of crystals on a single-crystal surface that determines their orientation. Epitaxy can be used to produce films and nanostructures of materials with a level of perfection that approaches that of single crystals. It may be used to produce materials that cannot be grown as large single crystals due to either economic or technical constraints. Epitaxial growth is typically limited to ultrahigh vacuum (UHV) techniques such as molecular beam epitaxy and other vapor deposition methods. In this Account, we will discuss the use of electrodeposition to produce epitaxial films of inorganic materials in aqueous solution under ambient conditions. In addition to lower capital costs than UHV deposition, electrodeposition offers additional levels of control due to solution additives that may adsorb on the surface, solution pH, and, especially, the applied overpotential. We show, for instance, that chiral morphologies of the achiral materials CuO and calcite can be produced by electrodepositing the materials in the presence of chiral agents such as tartaric acid.

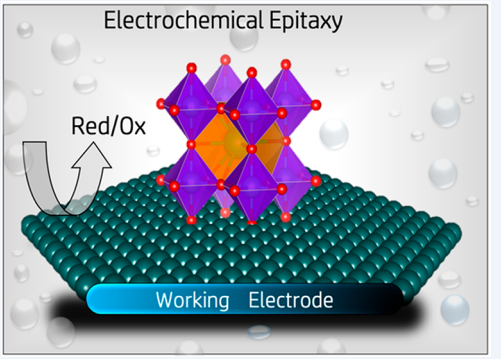

Inorganic compound materials are electrodeposited by an electrochemical-chemical mechanism in which solution precursors are electrochemically oxidized or reduced in the presence of molecules or ions that react with the redox product to form an insoluble species that deposits on the electrode surface. We present examples of reaction schemes for the electrodeposition of transparent hole conductors such as CuI and CuSCN, the magnetic material Fe_3O_4, oxygen evolution catalysts such as $Co(OH)_2$, CoOOH, and Co_3O_4, and the n-type semiconducting oxide ZnO. These materials can all be electrodeposited as epitaxial films or nanostructures onto single-crystal surfaces. Examples of epitaxial growth are given for the growth of films of CuI(111) on Si(111) and nanowires of CuSCN(001) on Au(111). Both are large mismatch systems, and the epitaxy is explained by invoking coincidence site lattices in which x unit meshes of the film overlap with y unit meshes of the substrate.

We also discuss the epitaxial lift-off of single-crystal-like foils of metals such as Au(111) and Cu(100) that can be used as flexible substrates for the epitaxial growth of semiconductors. The metals are grown on a Si wafer with a sacrificial SiO_x interlayer that can be removed by chemical etching. The goal is to move beyond the planar structure of conventional Si-based chips to produce flexible electronic devices such as wearable solar cells, sensors, and flexible displays. A scheme is shown for the epitaxial lift-off of wafer-scale foils of the transparent hole conductor CuSCN.

Finally, we offer some perspectives on possible future work in this area. One question we have not answered in our previous work is whether these epitaxial films and nanostructures can be grown with the level of perfection that is achieved in UHV. Another area that is ripe for exploration is the epitaxial electrodeposition of metal−organic framework materials from solution precursors.

KEY REFERENCES

- Switzer, J. A.; Shumsky, M. G.; Bohannan, E. W. Electrodeposited ceramic single crystals. *Science* **1999**, *284*, (5412), 293−296.[1] *This was our first example of epitaxial electrodeposition. δ-Bi_2O_3 is a high oxide mobility material that is normally only stable from 729 to 825 °C. It is electrodeposited from aqueous solution onto single-crystal Au substrates.*
- Switzer, J. A.; Kothari, H. M.; Poizot, P.; Nakanishi, S.; Bohannan, E. W. Enantiospecific electrodeposition of a chiral catalyst. *Nature* **2003**, *425*, (6957), 490−493.[2] *CuO is an achiral material in the bulk. We show that epitaxial films of CuO can be electrodeposited with a*

Received: January 5, 2023
Published: April 24, 2023

surface chirality that is controlled by chiral tartrate ions in solution.

- Mahenderkar, N. K.; Chen, Q.; Liu, Y.-C.; Duchild, A. R.; Hofheins, S.; Chason, E.; Switzer, J. A. Epitaxial lift-off of electrodeposited single-crystal gold foils for flexible electronics. *Science* **2017**, *355*, 1203−1206.[3] *We introduce a simple and inexpensive procedure to produce highly ordered flexible and transparent foils of Au at the wafer scale by epitaxial lift-off from a silicon wafer.*
- Banik, A.; Tubbesing, J. Z.; Luo, B.; Zhang, X.; Switzer, J. A. Epitaxial Electrodeposition of Optically Transparent Hole-Conducting CuI on n-Si(111). *Chem. Mater.* **2021**, *33*, (9), 3220−3227.[4] *CuI is a wide bandgap p-type material used as a hole transport layer in organic and perovskite solar cells and LEDs. Epitaxial films of the material are electrodeposited onto n-Si(111) in spite of an interfacial layer of SiO_x.*

1. INTRODUCTION

Epitaxy is the growth of crystals on a single-crystal substrate that determines their orientation.[5,6] It can be used to produce films and nanostructures with a level of perfection that approaches that of single crystals. This is particularly important for electronic materials because grain boundaries can lead to deleterious effects such as lower carrier mobility and they can provide sites for electron−hole recombination. For other applications, such as structural materials, it may be desirable to intentionally produce defects in the material to improve the mechanical properties. Depending on the nucleation and growth modes, epitaxy can produce either an ensemble of crystals on the surface that all have the same in-plane and out-of-plane orientations, or a true single-crystal film that is oriented by the substrate. Epitaxy can also be used to tune the properties of materials through strain caused by lattice mismatch.[7] In ordered, porous materials such as metal organic frameworks (MOFs), epitaxy can be used to produce films with a unique pore size and with pores that are continuous through the entire film thickness.[8] In battery electrodes, crystallographic order can lead to higher capacities and faster charging times.[9,10] Although vapor deposition methods such as molecular-beam epitaxy (MBE) and chemical vapor deposition (CVD) have traditionally been used to deposit epitaxial films,[11−13] this Account will focus on using electrodeposition from aqueous solution under ambient conditions to produce epitaxial films of inorganic materials.

To the chemist, electrodeposition of epitaxial films seems simpler (and certainly less expensive) than ultrahigh vacuum (UHV) techniques. Materials are typically deposited in a beaker, using a relatively inexpensive potentiostat to control either the applied potential or current. Yet, there is a complexity that is not present in vacuum because of solution pH, speciation, additives, and the applied potential. This complexity can also lead to a richness in levels of control that may not be available in vacuum. For example, it has been shown that the shape and even the chirality of crystals of electrodeposited materials can be controlled through solution additives, pH, and applied potential.[2,14−16] Electrodeposition is unique among deposition methods in that the departure from equilibrium can be precisely controlled with millivolt precision (1 meV = $kT/25.7$) through the applied potential. The departure from equilibrium is the overpotential η and is defined as the difference between the applied potential E_{appl} and the equilibrium potential E_{equil}. We have previously used the overpotential to deposit nanoscale layered materials known as superlattices by simply pulsing the potential during deposition to control the composition or defect chemistry of the alternating layers.[17−20] A trade-off that must be made for this level of control is that substrates for epitaxial electrodeposition must be conducting or semiconducting and must be relatively stable in the deposition solution. Hence, the common use of noble metals such as Au as substrates. This constraint does limit the choices of substrates and films with low lattice mismatch.

The most obvious choice of materials to deposit as epitaxial films are metals because the reactions in which metal ions or complexes are reduced at an electrode surface are direct electrochemical reduction reactions.[21−24] Electroplating of metals is what comes to mind when one thinks of electrodeposition. We have followed a different path. We are interested in electrodepositing inorganic materials such as metal oxides,[1,16,25−33] metal hydroxides,[34−36] biominerals,[37] molecular framework materials,[38] and compound semiconductors and perovskites[4,39−41] as epitaxial films. Because the production of these materials by electrodeposition is not familiar to most readers, we will now detail the reaction schemes used to produce these inorganic materials, followed by a discussion of the epitaxial electrodeposition of ordered inorganic materials and the epitaxial lift-off of these films to produce single-crystal-like foils and membranes.

2. REACTION SCHEMES FOR ELECTRODEPOSITING INORGANIC MATERIALS

Inorganic compound materials are electrodeposited by an electrochemical-chemical mechanism in which solution precursors are electrochemically oxidized or reduced in the presence of molecules or ions that react with the redox product to form an insoluble species that deposits on the electrode surface. For the chemist, this is a challenging, yet satisfying, blend of inorganic chemistry, electrochemistry, and materials science. A generalized reaction scheme is shown in Figure 1. For transition-metal ions such as Cu(II), Fe(III), and Co(III)

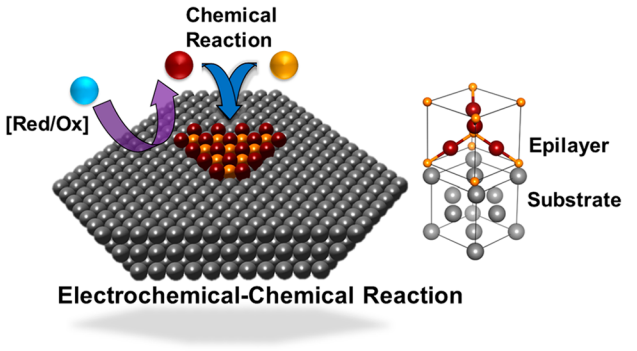

Figure 1. Electrochemical−Chemical reaction scheme used to produce epitaxial films and nanostructures of inorganic materials. Inorganic compounds are electrodeposited by a mechanism in which solution precursors are electrochemically oxidized or reduced (blue spheres to brown spheres) in the presence of molecules or ions (gold spheres) that react with the redox product to form an insoluble compound that deposits epitaxially on the electrode surface. By contrast, in metal electrodeposition a metal ion or complex is directly reduced to the metallic element without the subsequent chemical reaction.

https://doi.org/10.1021/acs.accounts.3c00007
Acc. Chem. Res. XXXX, XXX, XXX−XXX

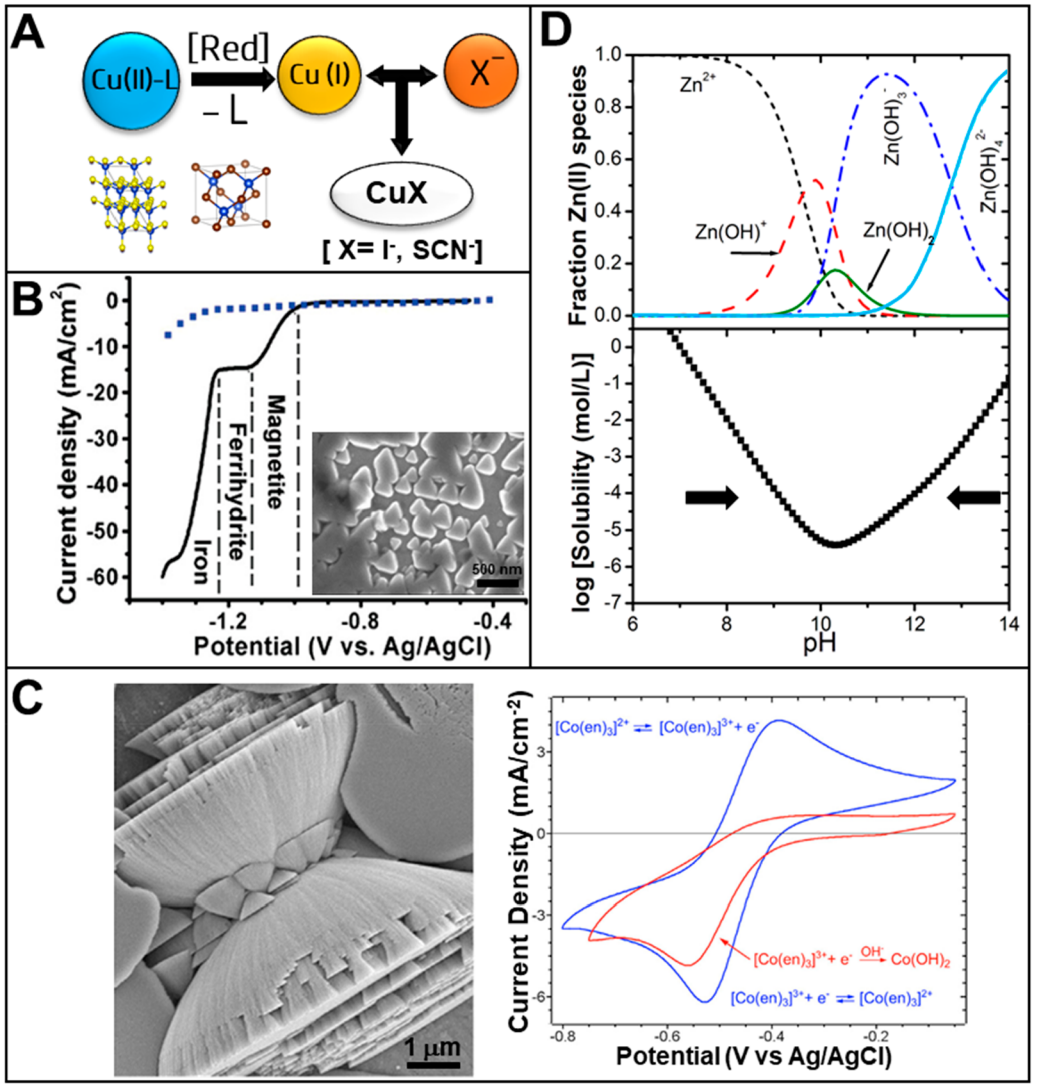

Figure 2. Examples of reactions used to produce inorganic materials. (A) Electrochemical reduction of complexes of Cu(II) in the presence of I^- or SCN^- to produce transparent hole conductors CuI and CuSCN. (B) Linear sweep voltammogram of Fe(III)-TEA complex in alkaline solution showing regions of stability for magnetite, ferrihydrite, and elemental iron. The inset shows an SEM micrograph of the initial stages of growth of single-domain magnetite on a Ni(111) single crystal. Adapted with permission from refs 30 and 44, Copyrights 2009 and 2011, American Chemical Society. (C) Cyclic voltammograms of $[Co(en)_3]^{3+}$ in a solution containing excess ethylenediamine (blue curve) and excess OH^- (red curve). In the alkaline solution, the complex is reduced irreversibly to β-$Co(OH)_2$. β-$Co(OH)_2$ is an active electrocatalyst for the oxygen evolution reaction. Reproduced with permission from ref 34, Copyright 2013, American Chemical Society. (D) Species of Zn(II) present and log(solubility) of Zn(II) as a function of pH. As indicated by the arrows on the solubility plot, amphoteric ZnO can be produced by generating base on the left-hand side of the diagram and by generating acid on the right-hand side of the diagram. ZnO is a large bandgap n-type semiconductor that grows as nanowires. Adapted with permission from ref 29, Copyright 2006, American Chemical Society.

that have variable oxidation states, the strategy is to use a ligand that forms a complex with the metal ion that is stable in solution, but upon oxidation or reduction a species is formed that is not strongly complexed and reacts with other molecules or ions in solution to produce the inorganic solid. For metal ions such as Zn(II) and Ca(II) that do not have soluble species with multiple oxidation states, the strategy is to use electrochemistry to oxidize or reduce another species in solution (including the solvent) that reacts with the ions to produce the solid. Specific examples of reaction schemes are shown in Figure 2.

An example of a metal ion with multiple accessible oxidation states is copper. Cu(II) is strongly complexed with ligands such as ethylenediaminetetraacetic acid (EDTA), tartrate ions, or lactate ions. However, when Cu(II) complexes are electrochemically reduced to Cu(I), the Cu^+ ion is available to react with other molecules or ions in solution. This is shown in the scheme in Figure 2A for the electrodeposition of the transparent hole conductors CuI and CuSCN.[4,39] If the Cu(II) is complexed with lactate or tartrate ions and reduced in an alkaline solution, the product will be insoluble Cu_2O, a p-type metal oxide semiconductor.[25,42,16,26,27] Another example of a material produced by this method is the magnetic material magnetite, Fe_3O_4. Figure 2B shows a linear sweep voltammogram of the complex of Fe(III) with the tripod ligand triethanolamine (TEA) in alkaline solution. Fe(III) is strongly complexed by TEA, but Fe^{2+} becomes available to react with OH^- in solution to form Fe_3O_4.[43] As shown in Figure 2B, the Fe_3O_4 is produced as the potential is driven negative of about −1 V versus Ag/AgCl.[30] The inset in Figure 2B shows the

https://doi.org/10.1021/acs.accounts.3c00007
Acc. Chem. Res. XXXX, XXX, XXX−XXX

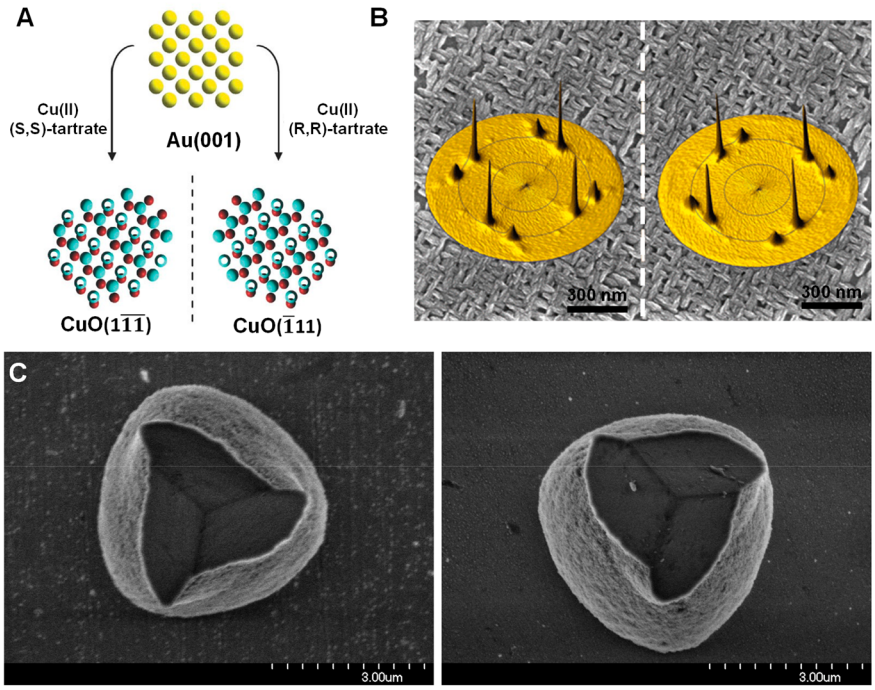

Figure 3. Examples of chiral electrodeposition. (A) CuO is electrodeposited onto Au(001) by the electrochemical oxidation of tartrate complexes of Cu(II). If the CuO is deposited using (*S*,*S*)-tartrate, CuO(1$\bar{1}\bar{1}$) is formed, but if it is deposited using (*R*,*R*)-tartrate CuO($\bar{1}$11) is formed. Both orientations lack mirror symmetry, and their mirror images are non-superimposable, consistent with 2D chirality. Reproduced with permission from ref 2, Copyright 2003, Springer Nature. (B) X-ray pole figures of the two CuO orientations, with an SEM micrograph of the CuO in background. Adapted with permission from ref 2, Copyright 2003, Springer Nature. (C) Chiral morphologies of calcite electrodeposited in the presence of *R*,*R*-tartaric acid (left panel) and *S*,*S*-tartaric acid (right panel). Reproduced with permission from ref 37, Copyright 2007, American Chemical Society.

initial stages of growth of epitaxial Fe_3O_4 on Ni(111). The Fe_3O_4 grows with the [111] orientation determined by the Ni(111) substrate and has a single in-plane domain.[44] At more negative potentials, ferrihydrite nanoribbons and finally elemental Fe are produced.[30] A final example of a material that is produced using a redox change of the metal ion is shown in Figure 2C, for the electrodeposition of $Co(OH)_2$. The synthesis exploits the fact that the kinetically inert Co(III) complex of ethylenediamine (en) is 35 orders of magnitude more stable than the kinetically labile Co(II) complex. $[Co(en)_3]^{3+}$ is therefore stable in alkaline solution, but $[Co(en)_3]^{2+}$ reacts with excess hydroxide ion to produce β-$Co(OH)_2$.[34] This is nicely shown in the cyclic voltammograms in Figure 2C. In the presence of excess ethylenediamine, the $[Co(en)_3]^{3+}$ exhibits a quasi-reversible reduction to $[Co(en)_3]^{2+}$ (blue curve in Figure 2C), but in the presence of excess OH^- the $[Co(en)_3]^{3+}$ is irreversibly reduced to β-$Co(OH)_2$ (red curve in Figure 2C). The scanning electron microscopy (SEM) micrograph in Figure 2C shows the unusual cone-shaped microstructure of the electrodeposited material. β-$Co(OH)_2$ can be electrochemically oxidized to CoOOH and thermally converted to Co_3O_4. All of these materials are potent electrocatalysts for the oxygen evolution reaction.[35,36]

An example of a material that can be produced by the electrochemical production of either acid or base is the n-type semiconductor ZnO (Figure 2D). ZnO and $Zn(OH)_2$ are amphoteric: they can dissolve in either acid or base. The top panel of Figure 2D shows the speciation diagram for Zn(II) as a function of pH. The metal ion is present as Zn^{2+} at low pH, then is progressively complexed by OH^- as the pH is increased. At approximately pH 10 the material precipitates as $Zn(OH)_2$ at room temperature but as ZnO at temperatures above 60 °C. As the pH is increased further, the soluble species $Zn(OH)_3^-$ and $Zn(OH)_4^{2-}$ are produced. The solubility of Zn(II) as a function of pH is shown in the bottom panel of Figure 2D. The arrows at low pH and at high pH show that the solubility limit can be reached by either producing base on the left-hand side of the diagram or producing acid on the right-hand side of the diagram. We have used both techniques to electrodeposit epitaxial ZnO nanowires on single-crystal Au.[28,29]

3. EPITAXIAL ELECTRODEPOSITION OF ORDERED INORGANIC MATERIALS

The ideal situation for epitaxial electrodeposition exists when the lattice mismatch between substrate and film is low. Although this occurs in epitaxial systems such as Au//Cu_2O in which the mismatch is 4.6%, many of the systems of interest have larger lattice mismatch. We have found that, even in these large mismatch systems, the orientation of the film can be templated by the substrate. These larger mismatch systems are often explained, or at least rationalized, by the formation of coincident site lattices (CSLs) in which *x* unit meshes of the film overlap with *y* unit meshes of the substrate or by rotation of the film relative to the substrate. The latter case is common among large mismatch systems on [100]-oriented substrates such as Cu(100) or Cu_2O(100) films on Si(100).[33,45] The epitaxial relationship between film and substrate is usually determined by X-ray diffraction (XRD). A standard θ-2θ X-ray pattern determines the out-of-plane orientation of the film relative to the substrate. The in-plane orientation of the film relative to the substrate is determined by X-ray pole figures using a four-circle diffractometer. In the X-ray pole figure, the

https://doi.org/10.1021/acs.accounts.3c00007
Acc. Chem. Res. XXXX, XXX, XXX−XXX

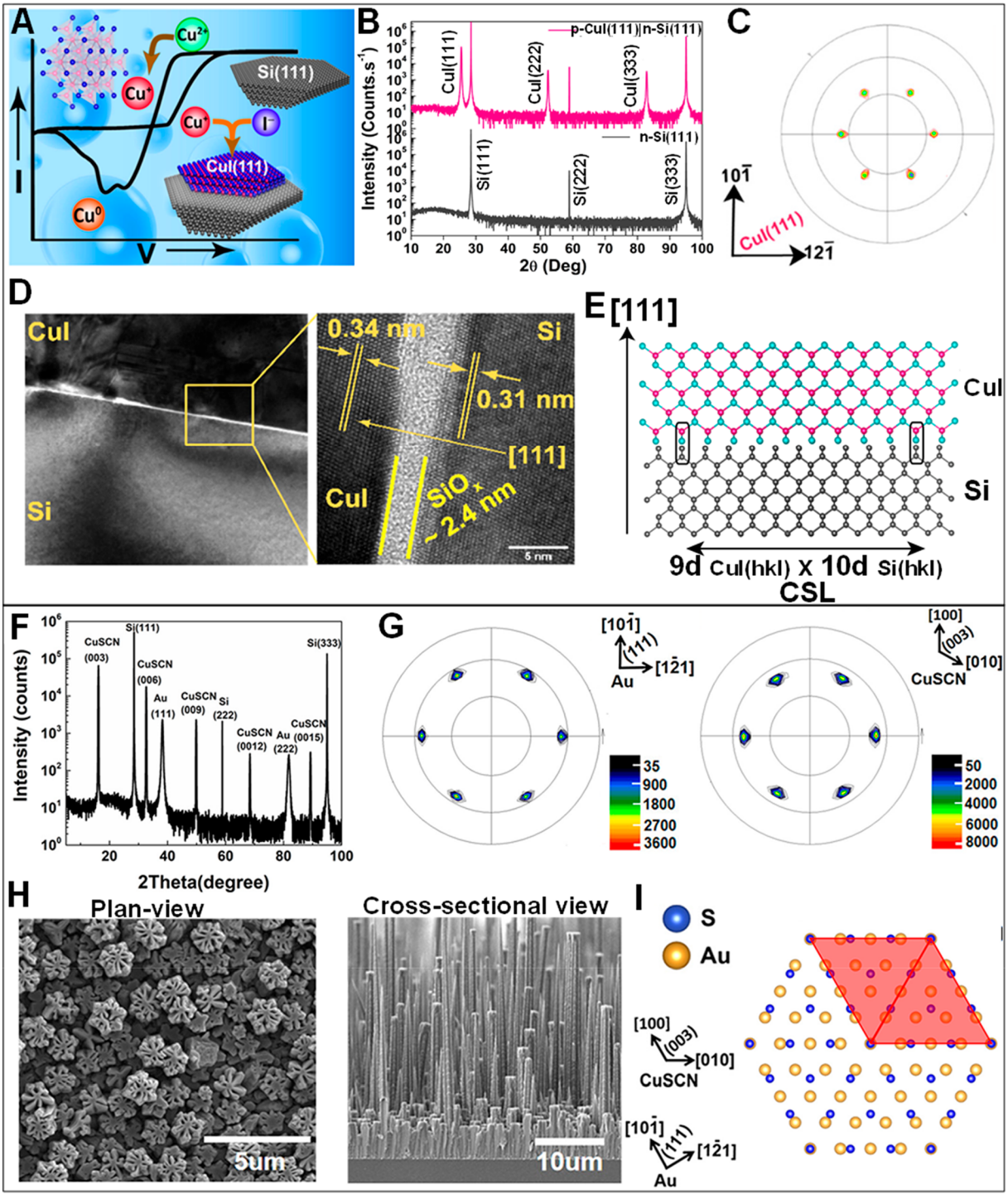

Figure 4. Epitaxial electrodeposition of the transparent hole conductors CuI and CuSCN. (A) Reaction scheme used to electrodeposit CuI. (B) X-ray diffraction pattern of CuI(111) on Si(111). (C) X-ray pole figure of CuI(111) on Si(111) showing in-plane order. (D) Cross-sectional TEM micrographs of CuI(111) on Si(111) showing 2.4 nm thick interfacial layer of SiO_x. (E) Interface model in which 9 unit meshes of CuI coincide with 10 unit meshes of Si. (A–E) Reproduced with permission from ref 4, Copyright 2021, American Chemical Society. (F) X-ray diffraction pattern of CuSCN(001) on Au(111). (G) X-ray pole figures of Au and CuSCN showing in-plane order. (H) Plan-view and cross-sectional SEM micrographs of CuSCN nanowires on Au(111). (I) Interface model in which 4 unit meshes of CuSCN coincide with 5 unit meshes of Au. (F–I) reproduced with permission from ref 39, Copyright 2022, American Chemical Society.

sample is tilted to bring planes into the Bragg condition that are not parallel with the geometric plane of the diffractometer. The sample is then rotated azimuthally to produce a two-dimensional (2D) spot pattern that is consistent with the symmetry of the plane being probed. The epitaxial relationship is then determined by comparing the spot pattern generated by the film to that generated by the substrate.

Although the substrate primarily determines the orientation of epitaxial films, complexing ligands can also have a profound effect. An interesting example is chiral electrodeposition. CuO

https://doi.org/10.1021/acs.accounts.3c00007
Acc. Chem. Res. XXXX, XXX, XXX−XXX

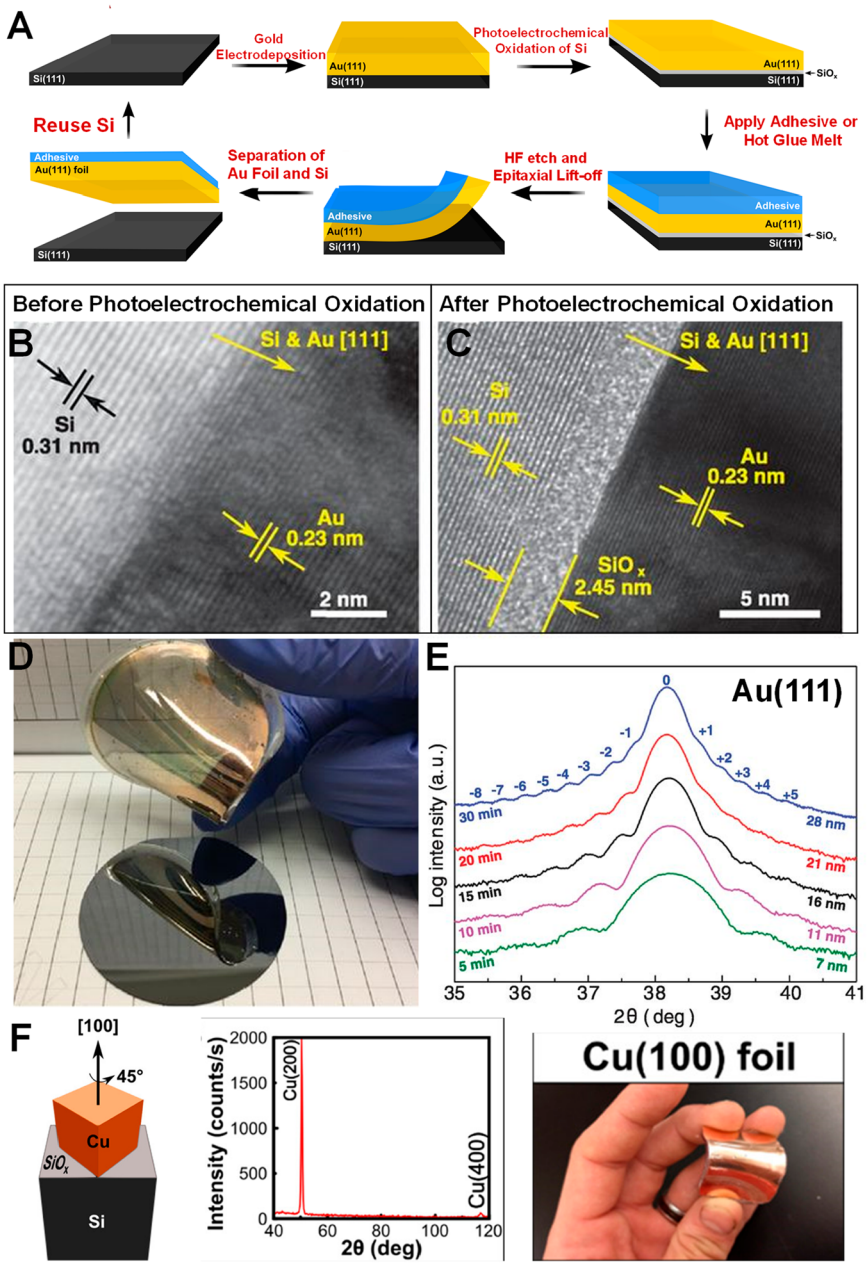

Figure 5. Epitaxial lift-off of Au(111) and Cu(100) single-crystal-like foils as substrates for flexible electronics. (A) Schematic of process used to produce Au(111) foils. (B) Cross-sectional TEM micrograph of epitaxial Au(111) on Si(111) showing the Au and Si in direct contact. (C) Cross-sectional TEM micrograph of epitaxial Au(111) on Si(111) after photo-electrochemical oxidation showing a 2.45 nm thick interfacial layer of SiO_x that is used as a sacrificial layer for lift-off. (D) Photograph of 28 nm thick Au(111) foil that was lifted off from a Si(111) wafer. (E) XRD patterns of Au(111) films of thicknesses ranging from 7 to 28 nm showing Laue oscillations that are an indication of the smoothness of the films. (A–E) Reproduced with permission from ref 3, Copyright 2017, The American Association for the Advancement of Science. (F) Schematic showing 45° rotation of Cu(100) relative to Si(100) in order to reduce lattice mismatch. XRD pattern showing [100] orientation for the Cu(100) foil that was lifted off of the Si(100). Optical micrograph of 175 nm thick, free-standing Cu(100) foil. Adapted with permission from ref 45, Copyright 2018, American Chemical Society.

and $CaCO_3$ are not intrinsically chiral materials: they do not crystallize in chiral space groups, and they do not exhibit bulk chiral effects such as the rotation of polarized light. Despite this lack of bulk chirality, biominerals based on calcite such as seashells crystallize into chiral morphologies. Two examples of earlier work from our group on chiral electrodeposition are shown in Figure 3. In the first case, CuO is electrodeposited onto Au(001) by electrochemically oxidizing tartrate complexes of Cu(II).[46] As shown in Figure 3A, if the CuO is deposited using (*S*,*S*)-tartrate CuO$(1\bar{1}\,\bar{1})$ is formed, but if is deposited using (*R*,*R*)-tartrate CuO$(\bar{1}11)$ is formed.[2] Both of these orientations lack mirror symmetry, and their mirror images are non-superimposable, consistent with 2D chirality. This is also demonstrated in the X-ray pole figures in Figure 3B (the background in this image is an SEM micrograph of the electrodeposited CuO). If the CuO is electrodeposited using a racemic mixture of the two enantiomorphs of tartrate, the X-ray pole figure shows mirror symmetry. Our attempt at

https://doi.org/10.1021/acs.accounts.3c00007
Acc. Chem. Res. XXXX, XXX, XXX−XXX

electrochemical biomineralization of chiral morphologies is shown in Figure 3C. Calcite is produced by electrochemically generating base by the reduction of water to H_2 to react with HCO_3^- in solutions containing Ca^{2+}. The CO_3^{2-} that is produced reacts with the Ca^{2+} to produce $CaCO_3$. If the calcite is electrodeposited in the presence of chiral molecules such as tartaric acid or the amino acid malic acid, a seashell-like spiral morphology is produced.[37] The calcite in the left panel of Figure 3 was produced in the presence of *R,R*-tartaric acid, and the calcite in the right panel was produced in the presence of *L,L*-tartaric acid. The *R,R*-tartaric acid produces calcite with a spiral that rotates to the left when viewed from above, whereas the *L,L*-tartaric acid produces calcite with a spiral that rotates to the right.

Our group has recently focused on the electrodeposition of wide-bandgap, transparent hole conductors such as CuI, CuBr, and CuSCN.[4,39,47] Data for epitaxial films and nanowires of CuI and CuSCN are shown in Figure 4. The bandgaps of CuI, CuBr, and CuSCN are 3.2, 3.1, and 3.85 eV, respectively. These transparent materials are used in organic and perovskite solar cells and light-emitting diodes (LEDs) to extract holes from the semiconductor. Although both the hole and electron conducting layers in these devices are typically polycrystalline, our work aims at the eventual goal of producing epitaxial architectures that minimize electron−hole recombination due to the lack of grain boundaries. The reaction scheme for depositing CuI(111) onto Si(111) is shown in Figure 4A.[4] An EDTA complex of Cu(II) is electrochemically reduced to produce Cu^+ in the presence of I^- at the Si(111) surface. As shown in Figure 4B, the electrodeposited CuI follows the [111] out-of-plane orientation of the Si(111). The pole figure in Figure 4C shows that the in-plane orientation of CuI is also determined by the Si(111). There are two in-plane domains of the CuI: one oriented parallel with respect to the Si and one oriented antiparallel with respect to the Si. In the antiparallel domain, the in-plane vectors of the film are rotated 180° with respect to those of the substrate. The epitaxial relations are given by $CuI(111)[12\bar{1}] \parallel Si(111)[12\bar{1}]$ and $CuI(111)[\bar{1}21] \parallel Si(111)[12\bar{1}]$. Because of the two in-plane domains, the CuI film could be described as single-crystal-like instead of single crystal. What is perhaps most surprising about the growth of CuI(111) on Si(111) is that the CuI is epitaxial in spite of a 2.4 nm thick interfacial layer of SiO_x, as shown in the cross-sectional transmission electron microscopy (TEM) micrographs in Figure 4D. SiO_x on Si is normally considered to be amorphous, so it is difficult to understand how the Si can template the epitaxial growth of the CuI. One explanation is that epitaxial CuI seed crystals are nucleated on the freshly etched n-Si(111) surface. Next, two processes take place simultaneously: surface oxidation of Si forming a thin layer of SiO_x and the lateral overgrowth of the CuI seeds into a continuous film. Another possible explanation is that the CuI nucleates on a very thin partially ordered SiO_x layer that forms initially. Researchers have shown by low-dosage scanning transmission electron microscopy (STEM) and surface X-ray diffraction that thermally grown SiO_x is partially crystalline.[48,49] Although the mismatch of CuI on Si is +11%, the epitaxy can be explained by invoking a CSL in which nine unit meshes of Cu coincide with ten unit meshes of Si. The mismatch of this CSL is only +0.02%.

The epitaxial growth of CuSCN nanowires on Au-coated Si(111) is shown in Figure 4F−I. The material is deposited by a similar mechanism to that used for CuI. Namely, a Cu(II) EDTA complex is electrochemically reduced in the presence of SCN^- ions.[39] For the substrate in this case we used a 28 nm thick film of [111]-oriented Au on Si(111) as an inexpensive proxy for single-crystal Au(111).[50] An X-ray pattern of the CuSCN on Au(111)//Si(111) is shown in Figure 4F. Only the (00l) reflections are observed in the pattern, showing a very strong [001] out-of-plane orientation. The epitaxial relationship determined from the pole figures in Figure 4G is $CuSCN(003)[100]//Au(111)[10\bar{1}]$. The CuSCN grows with a most unusual morphology as shown in Figure 4H. It initially deposits as a dense film, but after a few micrometers grows skyscraper-like nanowires. When viewed from the top, these nanowires have a snowflake-like structure. Again, this is a large mismatch system, but the epitaxy can be explained by a CSL in which 4 unit meshes of CuSCN(001) overlap with 5 unit meshes of Au(111) to produce a mismatch of only +0.22% (Figure 4I).

4. EPITAXIAL LIFT-OFF OF ORDERED FOILS FOR FLEXIBLE ELECTRONICS

Although perfect single-crystal substrates really shine for fundamental studies of epitaxial growth, they lose their luster when it comes to practical applications. We therefore sought an inexpensive alternative to single crystals of materials such as Au.[50] As an added benefit to this aspect of the work, we discovered a method to produce wafer-scale, single-crystal-like foils of metals such as Au(111) and Cu(100) that can be used as flexible substrates for the deposition of semiconductor materials such as Cu_2O and ZnO for flexible electronics.[3,45] This work was inspired by the research of Allongue and coworkers, who showed the unexpected result that very smooth epitaxial films of Au(111) can be electrodeposited onto Si(111) by depositing the Au at a negative enough potential to inhibit the growth of SiO_x on the Si.[51]

Figure 5A shows the scheme we have used to produce epitaxial films of Au(111) on Si(111) and the subsequent epitaxial lift-off to produce Au(111) foils.[3] The Au was electrodeposited onto Si(111) from a dilute $HAuCl_4$ solution at an applied potential of −1.9 V versus Ag/AgCl. The sample was then photo-electrochemically oxidized by irradiation in a solution of 0.5 M H_2SO_4 at a potential of +0.75 V versus Ag/AgCl to form a layer of SiO_x between the Au and Si. Finally, the SiO_x was etched in dilute HF solution, and the Au foil was separated from the Si. The initially deposited Au(111) was in direct contact with the Si(111) as shown in Figure 5B, but after photo-electrochemical oxidation of the Si, the Au was separated by a 2.45 nm thick film of SiO_x (Figure 5C), which served as a sacrificial layer for epitaxial lift-off. We refer to the Au films and foils as single-crystal-like, because there are parallel and antiparallel domains of Au(111) on the Si(111). The epitaxial relationships of these domains are given by $Au(111)[12\bar{1}] \parallel Si(111)[12\bar{1}]$ and $Au(111)[\bar{1}21] \parallel Si(111)[12\bar{1}]$. What is significant about these results is that single-crystal-like films and foils of Au can be produced at the wafer scale using a very small amount of the precious metal. The photograph of a wafer-size foil of Au(111) that is 28 nm thick is shown in Figure 5D. The films and foils are very smooth and can be grown to various thicknesses depending on the deposition time. Figure 5E shows XRD patterns of films grown to thicknesses from 7 to 28 nm thick. The satellite peaks around the Bragg peak are called Laue oscillations. They are caused by constructive and destructive interference of X-rays, and they are a testament to the smoothness of the films.

https://doi.org/10.1021/acs.accounts.3c00007
Acc. Chem. Res. XXXX, XXX, XXX−XXX

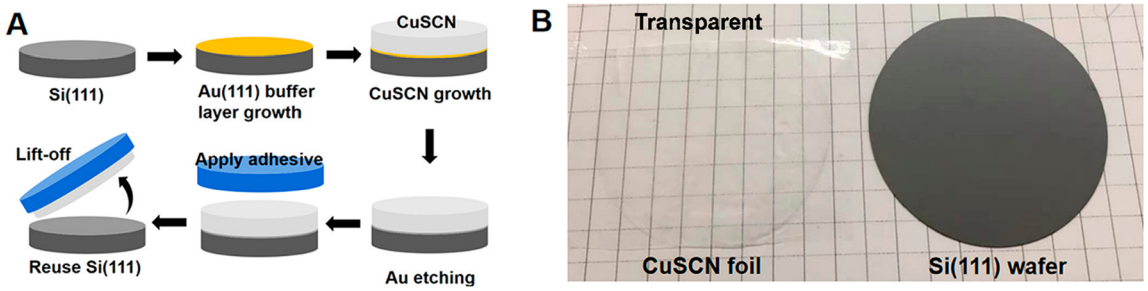

Figure 6. Epitaxial lift-off of wafer-scale foils of CuSCN(001). (A) Scheme used to deposit CuSCN(001) on Au(111) buffer layer on Si(111) and subsequent lift-off of CuSCN after triiodide etch of Au buffer layer. (B) Photograph of 400 nm thick transparent CuSCN(001) foil next to Si(111) wafer that was used as substrate for epitaxial lift-off. Reproduced with permission from ref 39, Copyright 2022, American Chemical Society.

A similar approach was used to produce foils of Cu(100) by depositing epitaxial films of Cu(100) on Si(100) and then removing the films as foils by epitaxial lift-off.[45] In this case, the photo-electrochemical oxidation was not necessary. The Cu(100) was deposited by nucleating epitaxial seeds of the Cu(100) at a potential of −1.5 V versus Ag/AgCl and then growing the film at a potential of −0.5 V versus Ag/AgCl. The sacrificial SiO_x layer formed during the growth cycle at more positive potentials. This is an interesting example of epitaxy, because the lattice mismatch between Cu and Si is −33.4%. The system lowers the mismatch to −5.9% by rotating the Cu 45° in-plane relative to the Si, as shown in Figure 5F. The single-domain, epitaxial relationship is Cu(100)[001] ‖ Si(100)[011]. An X-ray pattern of a 175 nm thick free-standing Cu(100) foil and a photograph of the foil are also shown in Figure 5F.

Epitaxial lift-off can also be used to produce flexible foils of semiconductors without the metal substrate. We have shown that flexible foils of the transparent hole conductor CuSCN can be produced using the scheme that is shown in Figure 6A.[39] A buffer layer of single-crystal-like Au(111) is deposited onto Si(111) followed by the electrodeposition of CuSCN(001) using the method outlined above. Although Au is normally considered to be inert, it can be etched using a triiodide etch, and the CuSCN(001) foil can be removed by epitaxial lift-off. A photograph of a 400 nm thick foil of CuSCN is shown in Figure 6B next to the 2 in. diameter Si wafer that was used to prepare the foil. The CuSCN foil is transparent due to the large bandgap of 3.85 eV.

5. CONCLUSIONS AND PERSPECTIVES

In this Account, we have outlined some schemes to produce inorganic materials by an electrochemical-chemical method. We have also given examples of epitaxial electrodeposition that include the formation of chiral surfaces, the electrodeposition of epitaxial transparent hole conductors, and the fabrication of single-crystal-like foils of metals and semiconductors for flexible electronics. We have also demonstrated that, although small lattice mismatch is preferred for the substrate and film, the substrate can still determine the out-of-plane and in-plane orientation of the epitaxial film for large mismatch systems.

Over a period of over two decades, we have electrodeposited a whole host of epitaxial systems. One question we have not answered is whether these electrodeposited films can have the same level of perfection that is observed in ultrahigh vacuum (UHV) techniques such as molecular beam epitaxy (MBE). For example, the films we electrodeposit typically have a larger mosaic spread (as measured by X-ray rocking curves) than those deposited in UHV. Also, for films deposited onto [111]-oriented cubic substrates, we often observe two in-plane domains. Is this an intrinsic limitation of electrodeposition due to the much lower processing temperatures? Although solid-state diffusion in these materials will be low, the mobility of ions on the surface can be quite high. With the proper choice of lattice mismatch, overpotential, organic additives, and preparation of the surface (such as the production of miscut, vicinal surfaces), it should be possible to deposit films as perfect as those grown in UHV. Vicinal surfaces and adsorbed molecules on the surface can break the surface symmetry to force the formation of a single in-plane domain. The formation of low-mismatch systems is a challenge because of the limited number of materials that can be used as substrates. This limitation might be circumvented, however, through remote epitaxy.[52,53] Remote epitaxy relaxes the constraint of low lattice mismatch by depositing a monolayer-thick layer of a van der Waals material such as graphene onto the surface. To our knowledge, this has not been applied to epitaxial electrodeposition.

Another area that is ripe for study is the epitaxial electrodeposition of metal−organic framework (MOF) materials from solution precursors. These porous materials have pore sizes that depend on the crystallographic orientation.[54−56] For example, the well-studied MOF Cu-BTC, where BTC is benzene-1,3,5-tricarboxylate, has 3.5 Å diameter pores along the [111] direction and 9.5 Å pores along the [100] direction.[54] If epitaxial films of this and other MOFs can be deposited, they will offer a unique pore size and will have open pores that run continuously through the film thickness. This will be ideal for chemical sensing, catalysis, and gas separation. Films of Cu-BTC have been produced electrochemically by oxidizing Cu in the presence of the BTC linker molecule.[57] The films formed by a dissolution−precipitation mechanism and were polycrystalline. A clever electrochemical-chemical deposition method of producing the MOFs from solution precursors should be possible that will produce epitaxial films. There are literally thousands of MOFs produced with a variety of metal ions and linker molecules, so the possibilities are endless.

AUTHOR INFORMATION

Corresponding Author

Jay A. Switzer − *Department of Chemistry and Graduate Center for Materials Research, Missouri University of Science and Technology, Rolla, Missouri 65409-1170, United States;* orcid.org/0000-0002-7332-4634; Email: jswitzer@mst.edu

https://doi.org/10.1021/acs.accounts.3c00007
Acc. Chem. Res. XXXX, XXX, XXX−XXX

Author

Avishek Banik − *Department of Chemistry and Graduate Center for Materials Research, Missouri University of Science and Technology, Rolla, Missouri 65409-1170, United States;* orcid.org/0000-0001-7269-1929

Complete contact information is available at: https://pubs.acs.org/10.1021/acs.accounts.3c00007

Author Contributions

CRediT: **Jay A. Switzer** conceptualization (lead), funding acquisition (lead), investigation (lead), project administration (lead), writing-original draft (lead), writing-review & editing (lead); **Avishek Banik** data curation (equal), visualization (lead), writing-original draft (supporting), writing-review & editing (equal).

Notes

The authors declare no competing financial interest.

Biographies

Jay A. Switzer is a Chancellor's Professor in the Chemistry Department and a Senior Investigator in the Materials Research Center at Missouri University of Science and Technology. He was born in Cincinnati, Ohio in 1950. J.A.S. received his B.S. in Chemistry from the University of Cincinnati and his Ph.D. in Inorganic Chemistry from Wayne State University, under the direction of John F. Endicott. Prior to moving to Missouri S&T in 1990 as a Professor, Switzer was a Senior Research Chemist at Union Oil Company of California (UNOCAL) working on semiconductor photoelectrochemistry, and an Associate Professor in the Materials Science and Engineering Department at the University of Pittsburgh. J.A.S. is a Fellow of AAAS, MRS, ECS, and JSPS. His research interests focus on inorganic materials chemistry and electrochemistry.

Avishek Banik received his Ph.D. in Chemistry in 2019 from Indian Institute of Technology Guwahati, India. A.B. was born in Assam, India, in 1988. A.B. is currently a postdoctoral research fellow in Jay A. Switzer's group at the Materials Research Center, Missouri University of Science and Technology, United States. His research focuses on epitaxial electrodeposition of inorganic materials for optoelectronics.

■ ACKNOWLEDGMENTS

J.A.S. would like to acknowledge the hard work and creativity of a large number of students and postdocs whose names appear in the references. Initial work on the electrodeposition of superlattices, epitaxial ceramics, and chiral films was supported by grants from the National Science Foundation. Research since the year 2008 was supported by the U.S. Department of Energy, Office of Basic Energy Sciences, Division of Materials Sciences and Engineering, under Grant No. DE-FG02-08ER46518.

■ REFERENCES

(1) Switzer, J. A.; Shumsky, M. G.; Bohannan, E. W. Electrodeposited ceramic single crystals. *Science* **1999**, *284* (5412), 293−296.
(2) Switzer, J. A.; Kothari, H. M.; Poizot, P.; Nakanishi, S.; Bohannan, E. W. Enantiospecific electrodeposition of a chiral catalyst. *Nature* **2003**, *425* (6957), 490−493.
(3) Mahenderkar, N. K.; Chen, Q.; Liu, Y.-C.; Duchild, A. R.; Hofheins, S.; Chason, E.; Switzer, J. A. Epitaxial lift-off of electrodeposited single-crystal gold foils for flexible electronics. *Science* **2017**, *355*, 1203−1206.
(4) Banik, A.; Tubbesing, J. Z.; Luo, B.; Zhang, X.; Switzer, J. A. Epitaxial Electrodeposition of Optically Transparent Hole-Conducting CuI on n-Si(111). *Chem. Mater.* **2021**, *33* (9), 3220−3227.
(5) Bauer, E. G.; Dodson, B. W.; Ehrlich, D. J.; Feldman, L. C.; Flynn, C. P.; Geis, M. W.; Harbison, J. P.; Matyi, R. J.; Peercy, P. S.; Petroff, P. M.; Phillips, J. M.; Stringfellow, G. B.; Zangwill, A. Fundamental issues in heteroepitaxy—A Department of Energy, Council on Materials Science Panel Report. *J. Mater. Res.* **1990**, *5* (4), 852−894.
(6) Stringfellow, G. B. Epitaxy. *Rep. Prog. Phys.* **1982**, *45* (5), 469−529.
(7) Bean, J. C. Strained-Layer Epitaxy of Germanium-Silicon Alloys. *Science* **1985**, *230* (4722), 127−131.
(8) Gu, Z.-G.; Zhang, J. Epitaxial growth and applications of oriented metal−organic framework thin films. *Coord. Chem. Rev.* **2019**, *378*, 513−532.
(9) Zahiri, B.; Patra, A.; Kiggins, C.; Yong, A. X. B.; Ertekin, E.; Cook, J. B.; Braun, P. V. Revealing the role of the cathode−electrolyte interface on solid-state batteries. *Nat. Mater.* **2021**, *20* (10), 1392−1400.
(10) Zheng, J.; Zhao, Q.; Tang, T.; Yin, J.; Quilty, C. D.; Renderos, G. D.; Liu, X.; Deng, Y.; Wang, L.; Bock, D. C.; Jaye, C.; Zhang, D.; Takeuchi, E. S.; Takeuchi, K. J.; Marschilok, A. C.; Archer, L. A. Reversible epitaxial electrodeposition of metals in battery anodes. *Science* **2019**, *366* (6465), 645−648.
(11) Panish, M. B. Molecular Beam Epitaxy. *Science* **1980**, *208* (4446), 916−922.
(12) Inagaki, S.; Nakamura, M.; Aizawa, N.; Peng, L.; Yu, X.; Tokura, Y.; Kawasaki, M. Molecular beam epitaxy of high-quality CuI thin films on a low temperature grown buffer layer. *Appl. Phys. Lett.* **2020**, *116* (19), 192105.
(13) Kampmeier, J.; Borisova, S.; Plucinski, L.; Luysberg, M.; Mussler, G.; Grützmacher, D. Suppressing Twin Domains in Molecular Beam Epitaxy Grown Bi_2Te_3 Topological Insulator Thin Films. *Cryst. Growth Des.* **2015**, *15* (1), 390−394.
(14) Switzer, J. A.; Kothari, H. M.; Bohannan, E. W. Thermodynamic to Kinetic Transition in Epitaxial Electrodeposition. *J. Phys. Chem. B* **2002**, *106* (16), 4027−4031.
(15) Choi, K.-S. Shape control of inorganic materials via electrodeposition. *Dalton Trans* **2008**, No. 40, 5432−5438.
(16) Liu, R.; Oba, F.; Bohannan, E. W.; Ernst, F.; Switzer, J. A. Shape control in epitaxial electrodeposition: Cu_2O nanocubes on InP(001). *Chem. Mater.* **2003**, *15* (26), 4882−4885.
(17) Switzer, J. A.; Shane, M. J.; Phillips, R. J. Electrodeposited ceramic superlattices. *Science* **1990**, *247* (4941), 444−446.
(18) Switzer, J. A.; Hung, C. J.; Breyfogle, B. E.; Shumsky, M. G.; Van Leeuwen, R.; Golden, T. D. Electrodeposited defect chemistry superlattices. *Science* **1994**, *264* (5165), 1573−1576.
(19) He, Z.; Koza, J. A.; Mu, G.; Miller, A. S.; Bohannan, E. W.; Switzer, J. A. Electrodeposition of $Co_xFe_{3-x}O_4$ Epitaxial Films and Superlattices. *Chem. Mater.* **2013**, *25* (2), 223−232.
(20) Switzer, J. A.; Gudavarthy, R. V.; Kulp, E. A.; Mu, G.; He, Z.; Wessel, A. J. Resistance Switching in Electrodeposited Magnetite Superlattices. *J. Am. Chem. Soc.* **2010**, *132* (4), 1258−1260.
(21) Liu, Y.; Gokcen, D.; Bertocci, U.; Moffat, T. P. Self-terminating growth of platinum films by electrochemical deposition. *Science* **2012**, *338*, 1327−1330.
(22) Mallett, J. J.; Svedberg, E. B.; Vaudin, M. D.; Bendersky, L. A.; Shapiro, A. J.; Egelhoff, W. F.; Moffat, T. P. Electrodeposited epitaxial $Fe_{100-x}Co_x$ films on n-GaAs(100). *Phys. Rev. B* **2007**, *75* (8), 085304.
(23) Sieradzki, K.; Brankovic, S. R.; Dimitrov, N. Electrochemical Defect-Mediated Thin-Film Growth. *Science* **1999**, *284* (5411), 138−141.
(24) Yang, F. Y.; Liu, K.; Hong, K.; Reich, D. H.; Searson, P. C.; Chien, C. L. Large Magnetoresistance of Electrodeposited Single-Crystal Bismuth Thin Films. *Science* **1999**, *284* (5418), 1335−1337.
(25) Bohannan, E. W.; Shumsky, M. G.; Switzer, J. A. Epitaxial Electrodeposition of Copper(I) Oxide on Single-Crystal Gold(100). *Chem. Mater.* **1999**, *11* (9), 2289−2291.

(26) Liu, R.; Bohannan, E. W.; Switzer, J. A.; Oba, F.; Ernst, F. Epitaxial electrodeposition of Cu_2O films onto InP(001). *Appl. Phys. Lett.* **2003**, *83* (10), 1944−1946.
(27) Liu, R.; Kulp, E. A.; Oba, F.; Bohannan, E. W.; Ernst, F.; Switzer, J. A. Epitaxial Electrodeposition of High-Aspect-Ratio Cu_2O(110) Nanostructures on InP(111). *Chem. Mater.* **2005**, *17* (4), 725−729.
(28) Liu, R.; Vertegel, A. A.; Bohannan, E. W.; Sorenson, T. A.; Switzer, J. A. Epitaxial electrodeposition of zinc oxide nanopillars on single-crystal gold. *Chem. Mater.* **2001**, *13* (2), 508−512.
(29) Limmer, S. J.; Kulp, E. A.; Switzer, J. A. Epitaxial Electrodeposition of ZnO on Au(111) from Alkaline Solution: Exploiting Amphoterism in Zn(II). *Langmuir* **2006**, *22* (25), 10535−10539.
(30) Kulp, E. A.; Kothari, H. M.; Limmer, S. J.; Yang, J.; Gudavarthy, R. V.; Bohannan, E. W.; Switzer, J. A. Electrodeposition of Epitaxial Magnetite Films and Ferrihydrite Nanoribbons on Single-Crystal Gold. *Chem. Mater.* **2009**, *21* (21), 5022−5031.
(31) Koza, J. A.; He, Z.; Miller, A. S.; Switzer, J. A. Electrodeposition of Crystalline Co_3O_4- A Catalyst for the Oxygen Evolution Reaction. *Chem. Mater.* **2012**, *24* (18), 3567−3573.
(32) Oba, F.; Ernst, F.; Yu, Y.; Liu, R.; Kothari, H. M.; Switzer, J. A. Epitaxial growth of cuprous oxide electrodeposited onto semiconductor and metal substrates. *J. Am. Ceram. Soc.* **2005**, *88* (2), 253−270.
(33) Switzer, J. A.; Liu, R.; Bohannan, E. W.; Ernst, F. Epitaxial Electrodeposition of a Crystalline Metal Oxide onto Single-Crystalline Silicon. *J. Phys. Chem. B* **2002**, *106* (48), 12369−12372.
(34) Koza, J. A.; Hull, C. M.; Liu, Y.-C.; Switzer, J. A. Deposition of β-$Co(OH)_2$ Films by Electrochemical Reduction of Tris-(ethylenediamine)cobalt(III) in Alkaline Solution. *Chem. Mater.* **2013**, *25* (9), 1922−1926.
(35) Hull, C. M.; Koza, J. A.; Switzer, J. A. Electrodeposition of Epitaxial $Co(OH)_2$ and Conversion to Epitaxial CoOOH and Co_3O_4. *J. Mater. Res.* **2016**, *31*, 3324−3331.
(36) Liu, Y.-C.; Koza, J. A.; Switzer, J. A. Conversion of electrodeposited $Co(OH)_2$ to CoOOH and Co_3O_4, and comparison of their catalytic activity for the oxygen evolution reaction. *Electrochim. Acta* **2014**, *140*, 359−365.
(37) Kulp, E. A.; Switzer, J. A. Electrochemical Biomineralization: The Deposition of Calcite with Chiral Morphologies. *J. Am. Chem. Soc.* **2007**, *129* (49), 15120−15121.
(38) Nakanishi, S.; Lu, G.; Kothari, H. M.; Bohannan, E. W.; Switzer, J. A. Epitaxial Electrodeposition of Prussian Blue Thin Films on Single-Crystal Au(110). *J. Am. Chem. Soc.* **2003**, *125* (49), 14998−14999.
(39) Luo, B.; Banik, A.; Bohannan, E. W.; Switzer, J. A. Epitaxial Electrodeposition of Hole Transport CuSCN Nanorods on Au(111) at the Wafer Scale and Lift-off to Produce Flexible and Transparent Foils. *Chem. Mater.* **2022**, *34* (3), 970−978.
(40) Banik, A.; Bohannan, E. W.; Switzer, J. A. Epitaxial Electrodeposition of BiI_3 and Topotactic Conversion to Highly-Ordered Solar Light Absorbing Perovskite $(CH_3NH_3)_3Bi_2I_9$. *Chem. Mater.* **2020**, *32*, 8367−8372.
(41) Koza, J. A.; Hill, J. C.; Demster, A. C.; Switzer, J. A. Epitaxial electrodeposition of methylammonium lead iodide perovskites. *Chem. Mater.* **2016**, *28* (1), 399−405.
(42) Golden, T. D.; Shumsky, M. G.; Zhou, Y.; VanderWerf, R. A.; Van Leeuwen, R. A.; Switzer, J. A. Electrochemical deposition of copper(I) oxide films. *Chem. Mater.* **1996**, *8* (10), 2499−2504.
(43) Kothari, H. M.; Kulp, E. A.; Limmer, S. J.; Poizot, P.; Bohannan, E. W.; Switzer, J. A. Electrochemical deposition and characterization of Fe_3O_4 films produced by the reduction of Fe(III)-triethanolamine. *J. Mater. Res.* **2006**, *21* (1), 293−301.
(44) Gudavarthy, R. V.; Gorantla, S.; Mu, G.; Kulp, E. A.; Gemming, T.; Eckert, J.; Switzer, J. A. Epitaxial Electrodeposition of Fe_3O_4 on Single-Crystal Ni(111). *Chem. Mater.* **2011**, *23* (8), 2017−2019.
(45) Hull, C. M.; Switzer, J. A. Electrodeposited Epitaxial Cu(100) on Si(100) and Lift-off of Single Crystal-Like Cu(100) Foils. *ACS Appl. Mater. Interfaces* **2018**, *10*, 38596−38602.
(46) Poizot, P.; Hung, C.-J.; Nikiforov, M. P.; Bohannan, E. W.; Switzer, J. A. An electrochemical method for CuO thin film deposition from aqueous solution. *Electrochem. Solid-State Lett.* **2003**, *6* (2), C21−C25.
(47) Luo, B.; Zhang, X.; Tubbesing, J. Z.; Banik, A.; Switzer, J. A. Epitaxial Electrodeposition of Wide Bandgap Cuprous Bromide on Silver via a Silver Bromide Buffer Layer. *J. Electrochem. Soc.* **2022**, *169* (9), 092512.
(48) Kimoto, K.; Tanaka, H.; Matsushita, D.; Tatsumura, K.; Takeno, S. Metastable ultrathin crystal in thermally grown SiO_2 film on Si substrate. *AIP Adv.* **2012**, *2* (4), 042144.
(49) Takahashi, I.; Shimura, T.; Harada, J. X-ray diffraction evidence for epitaxial microcrystallinity in thermally oxidized SiO_2 thin films on the Si(001) surface. *J. Phys.: Condens. Matter* **1993**, *5* (36), 6525.
(50) Switzer, J. A.; Hill, J. C.; Mahenderkar, N. K.; Liu, Y.-C. Nanometer-thick gold on silicon as a proxy for single-crystal gold for the electrodeposition of epitaxial cuprous oxide thin films. *ACS Appl. Mater. Interfaces* **2016**, *8* (24), 15828−15837.
(51) Prod'homme, P.; Maroun, F.; Cortes, R.; Allongue, P. Electrochemical growth of ultraflat Au(111) epitaxial buffer layers on H-Si(111). *Appl. Phys. Lett.* **2008**, *93* (17), 171901.
(52) Kim, Y.; Cruz, S. S.; Lee, K.; Alawode, B. O.; Choi, C.; Song, Y.; Johnson, J. M.; Heidelberger, C.; Kong, W.; Choi, S.; Qiao, K.; Almansouri, I.; Fitzgerald, E. A.; Kong, J.; Kolpak, A. M.; Hwang, J.; Kim, J. Remote epitaxy through graphene enables two-dimensional material-based layer transfer. *Nature* **2017**, *544* (7650), 340−343.
(53) Kim, H.; Chang, C. S.; Lee, S.; Jiang, J.; Jeong, J.; Park, M.; Meng, Y.; Ji, J.; Kwon, Y.; Sun, X.; Kong, W.; Kum, H. S.; Bae, S.-H.; Lee, K.; Hong, Y. J.; Shi, J.; Kim, J. Remote epitaxy. *Nat. Rev. Methods Primers* **2022**, *2* (1), 40.
(54) Chui, S. S.-Y.; Lo, S. M.-F.; Charmant, J. P. H.; Orpen, A. G.; Williams, I. D. A Chemically Functionalizable Nanoporous Material $[Cu_3(TMA)_2(H_2O)_3]_n$. *Science* **1999**, *283* (5405), 1148−1150.
(55) Furukawa, H.; Cordova, K. E.; O'Keeffe, M.; Yaghi, O. M. The Chemistry and Applications of Metal-Organic Frameworks. *Science* **2013**, *341* (6149), 1230444.
(56) Farha, O. K.; Eryazici, I.; Jeong, N. C.; Hauser, B. G.; Wilmer, C. E.; Sarjeant, A. A.; Snurr, R. Q.; Nguyen, S. T.; Yazaydın, A. Ö.; Hupp, J. T. Metal−Organic Framework Materials with Ultrahigh Surface Areas: Is the Sky the Limit? *J. Am. Chem. Soc.* **2012**, *134* (36), 15016−15021.
(57) Campagnol, N.; Van Assche, T. R. C.; Li, M.; Stappers, L.; Dincă, M.; Denayer, J. F. M.; Binnemans, K.; De Vos, D. E.; Fransaer, J. On the electrochemical deposition of metal−organic frameworks. *J. Mater. Chem. A* **2016**, *4* (10), 3914−3925.

NOTE ADDED AFTER ASAP PUBLICATION

This paper originally published ASAP on April 24, 2023. Due to a production error, a few minor corrections were made and a new version reposted on April 25, 2023.

https://doi.org/10.1021/acs.accounts.3c00007
Acc. Chem. Res. XXXX, XXX, XXX−XXX